

## Partition-Function Zeros and the SU(3) Deconfining Phase Transition

Nelson A. Alves,<sup>(1,2)</sup> Bernd A. Berg,<sup>(1,2)</sup> and Sergiu Sanielevici<sup>(1)</sup>

<sup>(1)</sup>Supercomputer Computations Research Institute, The Florida State University, Tallahassee, Florida 32306

<sup>(2)</sup>Department of Physics, The Florida State University, Tallahassee, Florida 32306

(Received 12 April 1990)

Using new methods to analyze Monte Carlo data, we have calculated the leading partition-function zero for SU(3) lattice gauge theory on various  $L_t L^3$  lattices. For  $L_t=4$  lattices we find in the range  $L=4-16$  the scaling behavior of a second-order transition with  $\nu=0.468(6)$ . However, for larger lattices ( $L=14-24$ ), the scaling behavior is consistent with a first-order transition:  $\nu=0.35(2)$ . The first-order nature of the transition is further substantiated by the fact that the finite-size scaling analysis of the specific heat yields a nonvanishing infinite-volume latent heat.

PACS numbers: 11.15.Ha, 12.38.Gc

If the finite-temperature phase transition between the hadronic and "plasma" phases of quantum chromodynamics (QCD) is first order, then the effects of this transition may be observable in heavy-ion collisions, cosmology, and astrophysics. Because of the nonperturbative character of the problem, numerical lattice simulations are the only systematic means to study it. In the limit of QCD where light quarks do not take part in the dynamics, the deconfining transition of the pure SU(3) theory had long been believed to be first order. Recently, criticism from the APE group<sup>1</sup> has shed some doubt on this belief. It now appears that the task of inferring the order of the deconfining transition from simulations on finite lattices is much more subtle than previously expected; see Ref. 2 for a review. Here we shed additional light on the issue by calculating the leading partition-function zeros for a number of  $L_t L^3$  lattices up to  $4 \times 24^3$ . Basically, this is achieved by following the approach of Refs. 3-5. However, reflecting the continuous nature of the SU(3) action density, we found it suitable to strictly avoid any use of histogramming. Essentially, this is achieved by keeping measurements (four double-precision numbers) after every sweep through the lattice, in this way filling up approximately a gigabyte disk. Subsequently, the measurements are analyzed and reweighting is done to construct the  $\beta$  dependence in appropriate small neighborhoods  $U(\beta_{MC})$  around the simulation values  $\beta_{MC}$ . A number of technical details will be reported elsewhere.<sup>6</sup> In this Letter we concentrate on the physics results.

Table I gives an overview of our most important final data. Each data point relies on at least 120000 Monte Carlo (MC) sweeps and measurements. Exceptions are the  $L=20$  lattices, where at  $\beta_{MC}=5.690$  and  $5.691$  we have 240000 sweeps and the two  $L=24$  lattices where we have 180000 sweeps in each case. An additional 10000 to 30000 sweeps were discarded for thermalization at the beginning of each run. For the MC updating we use the code of Ref. 7. The third and fourth columns of Table I collect our estimates for the real and imaginary parts of the partition-function zero closest to the real axis. (For the  $L=4$  lattice it is not the zero closest

to the real axis but the one selected by extrapolation from the lattices with larger spatial volume.) The fifth column gives the maximum for the variance of the average plaquette action,

$$\sigma^2(S_p) = \langle S_p^2 \rangle - \langle S_p \rangle^2 \quad \text{with} \quad S_p = \frac{1}{3} \text{Tr}(U_p), \quad (1)$$

searched for in the neighborhood of  $\beta_{MC}$  where reweighting is valid. The last column gives (without its error) the

TABLE I. Overview of  $L_t=4$  data.

$L_t \times L^3$	$\beta_{MC}$	$\beta_x^0$	$\beta_y^0$	$10^4 \sigma_{\max}^2(S_p)$	$\beta_{\max}$
$4 \times 4^3$	5.570	5.611(9)	0.204(12)	2.699(53)	5.443
$4 \times 4^3$	5.610	5.614(11)	0.209(13)	None	
$4 \times 4^3$	5.640	5.607(6)	0.185(6)	None	
$4 \times 6^3$	5.640	5.654(9)	Noise	0.591(10)	5.6390
$4 \times 6^3$	5.645	5.656(5)	0.0757(64)	0.619(22)	5.6132
$4 \times 6^3$	5.660	5.642(7)	0.0784(47)	None	
$4 \times 6^3$	5.690	5.645(8)	0.0801(80)	None	
$4 \times 8^3$	5.670	5.6747(23)	0.0466(27)	0.259(7)	5.6705
$4 \times 8^3$	5.693	5.6791(33)	0.0498(42)	0.249(7)	5.6772
$4 \times 10^3$	5.680	5.6889(14)	0.0301(18)	0.1407(53)	5.6878
$4 \times 10^3$	5.693	5.6864(55)	0.0280(81)	0.1350(39)	5.6839
$4 \times 12^3$	5.681	5.6934(17)	Bias	0.0923(55)	5.6908
$4 \times 12^3$	5.691	5.6896(17)	0.0203(7)	0.0952(28)	5.6890
$4 \times 14^3$	5.682	5.6886(18)	0.0143(9)	0.0651(30)	5.6882
$4 \times 14^3$	5.691	5.6922(13)	0.0138(7)	0.0713(35)	5.6924
$4 \times 16^3$	5.683	5.6904(16)	0.0101(10)	0.0492(32)	5.6904
$4 \times 16^3$	5.691	5.6918(10)	0.0101(6)	0.0529(26)	5.6923
$4 \times 16^3$	5.692	5.6917(10)	0.0096(5)	0.0547(23)	5.6917
$4 \times 20^3$	5.690	5.6917(6)	0.00554(22)	0.0386(17)	5.6916
$4 \times 20^3$	5.691	5.6915(6)	0.00527(17)	0.0399(16)	5.6916
$4 \times 20^3$	5.692	5.6929(7)	0.00531(28)	0.0386(22)	5.6931
$4 \times 24^3$	5.691	5.6931(7)	0.0027(2)	0.0404(70)	5.6932
$4 \times 24^3$	5.693	5.6913(9)	0.0032(4)	0.0306(25)	5.6911

corresponding  $\beta_{\max}$  value. In the case that the maximum is found on the boundary of  $U(\beta_{\text{MC}})$  "none" is entered in the fifth column. All our error are jackknife estimates; our estimators are corrected for bias by a "double-jackknife" method. Results from simulations at variant  $\beta_{\text{MC}}$  values are found to agree in a satisfactory way. It is remarkable that the only knowledge required for the results of Table I are the  $S_p$  distribution functions from the various MC runs, i.e., one number per measurement. In addition, we have measured the spacelike and timelike plaquette actions separately, as well as the real and imaginary parts of the Polyakov-loop expectation values. Results for these quantities, which seem to be less novel, will be reported in Ref. 6. The rest of this paper is devoted to the finite-size scaling analysis of the data presented in Table I.

To investigate the scaling behavior of the zero which is closest to the real  $\beta$  axis we follow the convention of Refs. 3 and 5 and introduce the variable  $u = e^{-\beta}$ , although complex  $\beta_0$  values could as well be used directly. For large  $L$  the imaginary part of the corresponding  $u^0$  zero scales like

$$|u_y^0| \sim L^{-1/\nu}. \tag{2}$$

(The real parts are too noisy to be useful for anything else but an estimate of the infinite-volume critical point  $\beta_c$ .) If the transition is first order, then we should find  $\nu = 1/d = 1/3$ . In Table II we collect the results of fits by Eq. (2) with varying ranges for  $L$ . For each fit the goodness of fit  $Q$  is monitored. For normally distributed data with known variances and under the assumption that the fit hypothesis is true,  $Q$  is uniformly distributed in the range  $0 < Q < 1$ . Clearly the  $L = 4-20$  and  $4-24$  fits have unacceptably small  $Q$ 's whereas all other fits are acceptable. In particular, it is remarkable that the entire range  $L = 4-16$  allows a consistent fit with  $\nu = 0.468(6)$  and that direct correlation length measurements<sup>9</sup> for lattices in the range  $L = 6-12$  give  $\nu = 0.473(19)$  with a still admissible  $Q = 0.09$ . Putting these two lines of results together, the illusion of a second-order transition is almost perfect. However, the  $L = 20$  results destroy the consistency of the fit and one has to conclude that true asymptotic behavior is only found for surprisingly large lattices. Investigating the consistency of fits for large lattices, one comes to the conclusion that the preferable

TABLE II. Fits of  $|u_y^0(L)|$ .

$L$ range	$\nu$	$Q$
4-14	0.475(7)	0.62
4-16	0.468(6)	0.19
4-20	0.451(5)	$8.9 \times 10^{-16}$
4-24	0.445(4)	$6.7 \times 10^{-10}$
14-24	0.35(2)	0.26
16-24	0.34(2)	0.14

breakpoint (with respect to  $Q$ ) is already at  $L = 14$ . Figure 1 gives a visual impression of the fits for  $L = 4-14$ , for  $L = 14-24$ , and for all  $L$ . Consequently, our final asymptotic large- $L$  results is

$$\nu = 0.35 \pm 0.02 \text{ from } L = 14-24 \text{ with } Q = 0.26. \tag{3}$$

As a test for the correctness as well as for the efficiency of our method we also simulated  $2 \times L^3$  lattices with  $L = 6, 8, 10$ , and  $12$  (120000 sweeps and measurements plus 10000 thermalization sweeps per data point). This calculation was completed in a few days; we obtained  $\nu = 0.331(5)$  with  $Q = 0.18$ . Thus, with little additional effort we confirm the result of Karliner, Sharpe, and Tang,<sup>10</sup> who report  $\nu = 0.331(6)$  from their more complicated constrained Monte Carlo calculation of partition-function zeros. It is amazing that for  $L_t = 2$  lattices the  $\nu$  estimate by fitting (2) is consistent with a first-order transition from the smallest volumes on, quite a contrast as compared to the  $L_t = 4$  lattices. A similar contrast was observed in a recent study of the surface tension in the deconfinement transition.<sup>11</sup>

A quantity which is easily calculated from the  $S_p$  distribution function is the reduced second moment (or variance)  $\sigma^2(S_p)$ . Frequently the fourth moment is invoked to distinguish a first- from a second-order transition. However, in Ref. 12 we observed that in the present case the fourth moment follows by the Gaussian relationship from the reduced second moment. (This relation continues to hold for the new  $L = 24$  lattices, although in this case the Kolmogorov tests<sup>12</sup> rule out that the distributions themselves are Gaussian.) Therefore, it is more straightforward to carry out a direct finite-size scaling analysis of the reduced second moment (1) or, equivalently, of the specific heat. The large- $L$  behavior

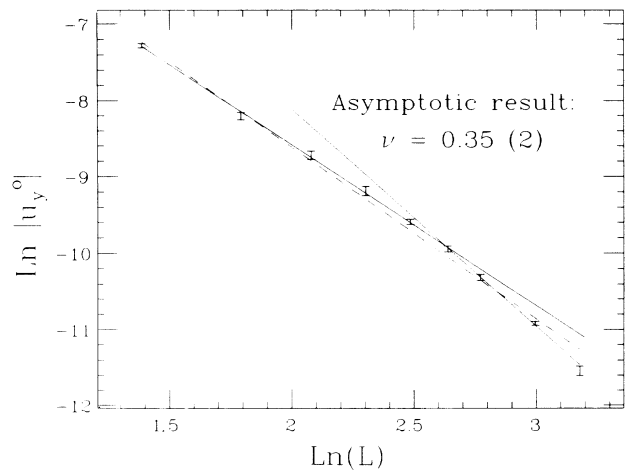


FIG. 1 Fits for  $\ln |u_y^0| = -(1/\nu) \ln(L)$ . The dashed line fits all data ( $Q = 6.7 \times 10^{-10}$ ). The first solid line corresponds to the range  $L = 4-14$  and the second, relevant for the asymptotic estimate of  $\nu$ , to the range  $L = 14-24$ .

is

$$\sigma^2(S_p) = a_1 L^{a/\nu-d} + a_2 L^{-d}. \quad (4a)$$

For a first-order phase transition,  $a/\nu = d$  and

$$\sigma^2(S_p) = a_1 + a_2 L^{-d}, \quad (4b)$$

where  $a_1$  is then related to the latent  $\Delta S_p$  of the average plaquette action  $S_p$  by

$$\Delta S_p = 2\sqrt{a_1}. \quad (5)$$

It is rather surprising that this relationship has not been exploited in previous investigations of the SU(3) deconfining transition. In Table III we collect the results of fits by Eq. (4b) with varying ranges for  $L$ . From  $L=6$  on, fits over the entire range of our lattices are consistent. The  $L=8-24$  fit is depicted in Fig. 2 and gives our final estimate of the latent heat,

$$\Delta S_p = (3.13 \pm 0.06) \times 10^{-3} \quad (6)$$

from  $L=8-24$  with  $Q=0.66$ .

In a frequently used notation, this translates to  $\Delta(\mathcal{E} - 3\mathcal{P})/T^4 = 4.02(9)$  in excellent agreement with values reported in Ref. 13 and well consistent with Ref. 14. Here  $\Delta\mathcal{E}$  is the latent heat and  $\mathcal{P}$  the pressure (continuous across the phase transition). Along the same lines we have also investigated  $\Delta(\mathcal{E} + \mathcal{P})$  which corresponds essentially to the difference of spacelike and timelike plaquettes, but in this case the signal barely allows us to determine the maximum of the variance and details are postponed to Ref. 6.

How do the approaches, zeros and specific heat, go together for small lattices? Let us assume that the hyperscaling relation<sup>15</sup>  $a = 2 - d\nu$  is valid. Then  $\nu$  determines  $a/\nu$  in Eq. (4a). Using the result  $\nu = 0.468(6)$  from the range  $L=4-16$  instead of  $\nu = 1/d$  as input, the resulting fit is already inconsistent for the range  $L=6-10$ :  $Q = 3.6 \times 10^{-14}$ . The fit for our whole  $L$  range is illustrated by the dashed curve in Fig. 2. In this way the small lattices tell us that the asymptotic behavior is not yet reached. Even more remarkably, assuming (4b) we learn from Table III that already rather small lattices ( $L=4-16$ ) give a reasonably good estimate of the infinite-volume latent heat. On the other hand, for  $L_t=2$  the two criteria give consistent answers already

TABLE III. Fits of  $\sigma^2(S_p)(L)$ .

$L$ range	$10^6 a_1$	$10^2 a_2$	$Q$
4-24	2.09(9)	1.29(2)	$10^{-38}$
6-24	2.35(9)	1.20(2)	0.18
8-24	2.45(10)	1.17(3)	0.66
10-24	2.47(12)	1.15(4)	0.56
8-16	2.50(17)	1.16(3)	0.41
10-14	2.59(27)	1.15(4)	0.26

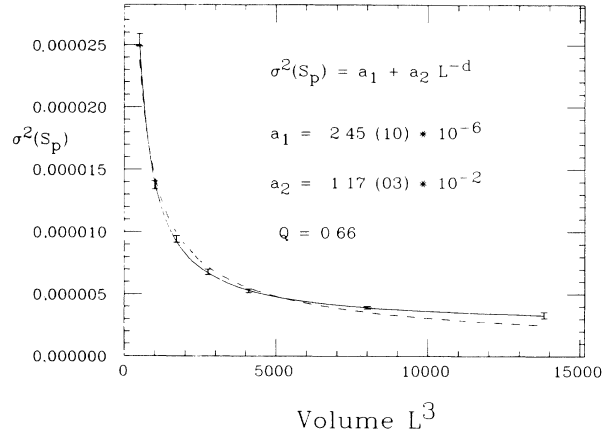


FIG. 2. Finite-size scaling estimate of the latent heat. The solid curve shows the fit using Eq. (4a), which leads to the displayed values of  $a_1$ ,  $a_2$ , and  $Q$ . The dashed curve shows the fit using (4b) with  $\nu=0.468$ .

from  $L=6$  on: Using  $\nu=0.331$  in Eq. (4a) gives an excellent fit to our  $L_t=2$  data for  $\sigma^2(S_p)$  ( $Q=0.61$ ).<sup>6</sup>

Putting both approaches together and assuming the validity of the hyperscaling relation we seem to arrive at a rather powerful method to distinguish numerically a first-order phase transition from a second-order one. If the two criteria give conflicting messages (as for  $L_t=4$  in the range  $L=4-16$ ), one obviously needs larger systems to settle the question of the order and the transition belongs in the twilight zone where the numerical methods do not allow us to distinguish a sufficiently strong second-order transition from a sufficiently weak first-order transition.

A nice feature of the approach proposed here that it does not rely on an order parameter but entirely on an analysis of the distribution function of the action. This should make the approach particularly suitable to full QCD, where the Polyakov loop ceases to be an order parameter.

The Monte Carlo data were produced on Florida State University's (FSU) ETA<sup>10</sup>s. In addition, this work would hardly have been possible without support by the FSU high-energy physics group through use of their gigabyte disks. In particular, we are indebted to Dennis Duke and Harvey Goldman. This research project was partially funded by the Department of Energy under Contracts No. DE-FG05-87ER40319 and No. DE-FC05-85ER2500. N.A. is supported by the Conselho Nacional de Desenvolvimento Científico e Tecnológico, Brazil.

<sup>1</sup>P. Bacilieri *et al.*, Phys. Rev. Lett. **61**, 1545 (1988); Phys. Lett. **B 224**, 333 (1989).

<sup>2</sup>A. Ukawa, in Proceedings of the International Symposium "Lattice '89," Capri, Italy [Nucl. Phys. B (Proc. Suppl.) (to be

published)].

<sup>3</sup>M. Falcioni, E. Marinari, M. L. Paciello, G. Parisi, and B. Taglienti, *Phys. Lett.* **108B**, 231 (1982); E. Marinari, *Nucl. Phys.* **B235 [FS11]**, 123 (1984).

<sup>4</sup>A. Ferrenberg and R. Swendsen, *Phys. Rev. Lett.* **61**, 2635 (1988).

<sup>5</sup>N. Alves, B. Berg, and R. Villanova, *Phys. Rev. B* **41**, 383 (1990).

<sup>6</sup>N. Alves, B. Berg, and S. Sanielevici (to be published).

<sup>7</sup>B. Berg, A. Devoto, and C. Vohwinkel, *Comp. Phys. Commun.* **51**, 331 (1988).

<sup>8</sup>W. Press *et al.*, *Numerical Recipes* (Cambridge Univ. Press, London, 1986).

<sup>9</sup>B. Berg, R. Villanova, and C. Vohwinkel, *Phys. Rev. Lett.*

**62**, 2433 (1989); B. Berg and N. Alves, in Proceedings of the International Symposium "Lattice '89," Capri, Italy (Ref. 2).

<sup>10</sup>M. Karliner, S. Sharpe, and Y. Chang, *Nucl. Phys.* **B302**, 204 (1988).

<sup>11</sup>S. Huang, J. Potvin, C. Rebbi, and S. Sanielevici, Boston University Report No. BUHEP-89-34 (unpublished).

<sup>12</sup>N. Alves, B. Berg, and S. Sanielevici, *Phys. Lett. B* (to be published).

<sup>13</sup>M. Fukugita, M. Okawa, and A. Ukawa, KEK Report No. KEK 89-73 (to be published).

<sup>14</sup>F. Brown, N. Christ, Y. Deng, M. Gao, and T. Woch, *Phys. Rev. Lett.* **61**, 2058 (1988).

<sup>15</sup>M. E. Fisher, in *Nobel Symposium 24*, edited by B. Lundquist and S. Lundquist (Academic, New York, 1974).